



Surface ozone at Nam Co (4730 m a.s.l.) in the inland Tibetan Plateau: variation, synthesis comparison and regional representativeness

Xiufeng Yin ^{1, 2, 3}, Shichang Kang ^{1, 4}, Benjamin de Foy ⁵, Zhiyuan Cong ^{2, 4}, Jiali Luo ⁶, Lang Zhang ², Yaoming Ma ^{2, 4}, Guoshuai Zhang ², Dipesh Rupakheti ^{2, 3}, Qianggong Zhang ^{2, 4}

¹State Key Laboratory of Cryosphere Sciences, Northwest Institute of Eco-Environment and Resources, Chinese Academy of Science, Lanzhou, 730000, China

²Key Laboratory of Tibetan Environment Changes and Land Surface Processes, Institute of Tibetan Plateau Research, Chinese Academy of Sciences, Beijing, 100101, China

³University of Chinese Academy of Sciences, Beijing, 100039, China

⁴CAS Center for Excellence in Tibetan Plateau Earth Sciences, Beijing, 100085, China

⁵Department of Earth and Atmospheric Sciences, Saint Louis University, St. Louis, MO, 63108, USA

⁶Key Laboratory of Semi-Arid Climate Change, Ministry of Education, Lanzhou, 730000, China

Correspondence to: Qianggong Zhang (qianggong.zhang@itpcas.ac.cn) and Shichang Kang (shichang.kang@lzb.ac.cn)

Abstract. Ozone is an important pollutant and greenhouse gas, and tropospheric ozone variations are generally associated with both natural and anthropogenic processes. As one of the most pristine and inaccessible regions in the world, the Tibetan Plateau has been considered as an ideal region for studying processes of the background atmosphere. Due to the vast area of the Tibetan Plateau, sites in the southern, northern and central regions exhibit different patterns of variation in surface ozone. Here, we present long-term measurements for ~5 years (January 2011 to October 2015) of surface ozone mixing ratios at Nam Co Station, which is a regional background site in the inland Tibetan Plateau. An average surface ozone mixing ratio of 47.6 ± 11.6 ppb was recorded, and a large annual cycle was observed with maximum ozone mixing ratios in the spring and minimum ratios during the winter. The diurnal cycle is characterized by a minimum in the early morning and a maximum in the late afternoon. Nam Co Station represents a background region where surface ozone receives negligible local anthropogenic emissions. Surface ozone at Nam Co Station is mainly dominated by natural processes involving photochemical reactions and potential local vertical mixing. Model results indicate that the study site is affected by the surrounding areas in different seasons and that air masses from the northern Tibetan Plateau lead to increased ozone levels in the summer. In contrast to the surface ozone levels at the edges of the Tibetan Plateau, those at Nam Co Station are less affected by stratospheric intrusions and human activities which makes Nam Co Station representative of vast background areas in the central Tibetan Plateau. By comparing measurements at Nam Co Station with those from other sites in the Tibetan Plateau and beyond, we aim to expand the understanding of ozone cycles and transport processes over the Tibetan Plateau. This work may provide a reference for model simulations in the future.



1 Introduction

The concentration of ozone in the troposphere showed sustained growth during the 20th century due to the increased emissions of anthropogenic precursors (Cooper et al., 2014). High levels of surface ozone are currently a major environmental concern because of the harm ozone poses to health and vegetation at the surface (Mauzerall and Wang, 2001; Desqueyroux et al., 2002). In addition, ozone is a major precursor of hydroxyl (OH) and hydroperoxy (HO₂) radicals and it controls the oxidation capacity of the atmosphere (Brasseur et al., 1999). Furthermore, as the third most important greenhouse gas (after carbon dioxide (CO₂) and methane (CH₄)), tropospheric ozone contributes to global warming and has an estimated globally average radiative forcing of $0.40 \pm 0.20 \text{ W m}^{-2}$ with high confidence level (Myhre et al., 2013).

The origin of tropospheric ozone and its temporal variation varies from site to site. Historically, the stratosphere was initially thought to be the main source of surface (tropospheric) ozone and a network of surface ozone monitoring sites was proposed (Junge, 1962). In the 1970s and 1980s, the effect of photochemical reactions in the troposphere on surface ozone became well recognized (Chameides and Walker, 1973; Crutzen, 1974) and photochemistry was identified as the dominant source of tropospheric ozone at some sites, as supported by models (Wu et al., 2007). Today, it is impossible to obtain a unified surface ozone mixing ratio that is representative of the entire world and a unified explanation for surface ozone variations at all sites is lacking. In this situation, background sites can represent areas with surface ozone concentrations that are under the control of largely uniform synoptic systems and are minimally affected by local anthropogenic sources. The study of surface ozone at background sites may enrich the understanding of surface ozone variation patterns.

Due to its small human population and low level of industrialization, the Tibetan Plateau is an ideal natural laboratory for studying surface ozone across remote regions of the Eurasian continent. Long term surface ozone measurements over the Tibetan Plateau have been conducted at Mt. Waliguan (northeast edge of the Tibetan Plateau) since 1994 (Xu et al., 2016), the Nepal Climate Observatory at Pyramid (NCO-P) which operates on the southern slope of the Himalayan region since 2006 (Cristofanelli et al., 2010) and the Xianggelila Regional Atmosphere Background Station at the southeastern rim of the Tibetan Plateau since 2007 (Ma et al., 2014). Analysis of long-term ozone mixing ratios at Waliguan Station has revealed steadily increasing concentrations over the past two decades (Xu et al., 2016) and has shown that maximum surface ozone occurs during the summer (Zhu et al., 2004). At NCO-P and Xianggelila, the downward transport of air masses from the stratosphere has been recognized as one of the most important natural inputs for troposphere ozone, and it results in a springtime maximum of surface ozone (Cristofanelli et al., 2010; Ma et al., 2014). It is noteworthy that these three monitoring sites are on the boundaries of the Tibetan Plateau. In the vast inland area of the Tibetan Plateau, surface ozone measurements were only



reported from Lhasa and Dangxiong for one year and two years, respectively. These measurements might be less representative
60 of regional surface ozone variation due to their proximity to human settlements and relatively short duration of the
measurements (Ran et al., 2014; Lin et al. 2015). The paucity of long-term surface ozone observations in the Tibetan Plateau,
especially in the inland region, limits our understanding of the regional background ozone level and the factors that influence
it and can potentially lead to inaccurate simulation of surface ozone variation over the Tibetan Plateau.

Surface ozone mixing ratios were monitored for ~5 years (January 2011 to October 2015) at Nam Co Station on the shore
65 of Nam Co Lake (30°30′-30°56′N, 90°16′-91°03′E). In this study, we investigated the seasonal and diurnal variations of surface
ozone and its influencing factors. We then evaluated surface ozone variability using combined observations over the Tibetan
Plateau and beyond. Finally, we discussed the potential representativeness of surface ozone at Nam Co as the regional
background of surface ozone in the inland Tibetan Plateau. This study expands the understanding of surface ozone variation
and transport processes that influence tropospheric ozone in the inland Tibetan Plateau, and it is potentially valuable for
70 assessing ozone-related climatic and environmental effects over the Tibetan Plateau.

2 Measurements and Methods

2.1 Measurement site

The Tibetan Plateau (27°N–45°N, 70°E–105°E, average elevation ~ 4 km) is the highest and most extensive highland in
the world and has been called the ‘Third Pole’ (Yao et al., 2012). The Nam Co Comprehensive Observation and Research
75 Station (hereafter referred to as the Nam Co Station, 30°46.44′N, 90°59.31′E, 4730 m a.s.l.) is a high altitude scientific research
center located between the southeast shore of Nam Co Lake (1 km from the station) and the foothills of the northern
Nyainqêntanglha Mountains (15 km from the station) in the southern-central region of the Tibetan Plateau (Fig. 1). Nam Co
Station was established to monitor atmospheric conditions in September 2005 and provided a long-term record of the
atmospheric environment in the Tibetan Plateau (Kang et al., 2011). Nam Co Station is in a natural flat field (220 × 100 m)
80 and records meteorological, ecological, and atmospheric data, including surface ozone mixing ratios (Cong et al., 2007; Li et
al., 2007; Huang et al., 2012; Liu et al., 2015; de Foy et al., 2016a). The climate at Nam Co Station is dry and cold, representing
a typical climate regime in the high mountain region. The solar radiation at Nam Co Station is stronger than that at other sites
at the same latitude due to the high altitude and thin air. Three synoptic systems influence the atmosphere at Nam Co Station:
The South Asian anticyclone (which controls the 100-hPa upper layer), a subtropical high-pressure system, and southeast warm
85 and wet airflow (during the monsoon season) (Qiao and Zhang, 1994). No major anthropogenic sources of atmospheric
emissions exist near Nam Co Station. The urban area closest to the station is Dangxiong County, which is located on the



southern slopes of the Nyainqêntanglha Mountain Range approximately 60 km south of Nam Co. Dangxiong is lower in elevation than Nam Co Station by more than 500 m. No large industries are located within 100 km of Nam Co Station. Local traffic is limited to a small number of vehicles traveling through the area during the tourist season.

90 2.2 Measurements: surface ozone and meteorology

The surface ozone mixing ratios were measured using a UV photometric instrument (Thermo Environmental Instruments, USA, Model 49i), which uses absorption of radiation at 254 nm and has a dual cell design. The ambient air inlet (Teflon tube) was 1.5 m above the roof and 4 m above the ground. The instrument has zero noise, 0.25 parts per billion (ppb) RMS (root mean square error) (60 s average time), a low detection limit of 0.5 ppb, a precision of 1 ppb and a response time of 20 s (10 s lag time). The change in sensitivity of the instrument was less than 2% over one year of observation. The instrument was calibrated using a 49i-PS calibrator (Thermo Environmental Instruments, USA) before measurements and during the monitoring periods. Field operators checked the instruments and created a monitoring log file every day. Due to the extreme winter weather that occurs at Nam Co, measurements were intermittently interrupted because of unstable power supply (due to damage from strong winds to the electrical wires) and equipment maintenance. All data displayed in this study are in UTC+8 (Beijing Time), and solar noon at Nam Co Station is at 13:56 in UTC+8.

Measurements of temperature, relative humidity, wind speed, wind direction and downward shortwave radiation (SWD) were conducted at Nam Co Station using an automatic weather station system (Milos520, Vaisala) and a radiation measurement system (CNR-1) (Ma et al., 2008).

2.3 Meteorological simulations

Gridded meteorological data for backward trajectories and Planetary boundary layer height (PBLH) were obtained from Global Data Assimilation System (GDAS-1) by the U.S. National Oceanic and Atmospheric Administration (NOAA) with $1^\circ \times 1^\circ$ latitude and longitude horizontal resolution and vertical levels of 23 from 1000 hPa to 20 hPa (<http://www.arl.noaa.gov/gdas1.php>).

Backward trajectories and clusters were calculated by NOAA-HYSPLIT (HYbrid Single-Particle Lagrangian Integrated Trajectory) model (Draxler and Rolph, 2003) using TrajStat, which is a free software plugin of Meteoinfo (Wang, 2014). The backward trajectories arrival height was set at 500 m above the surface and the total run times was 120 hours for each backward trajectory and in time interval of 3 hours. Angle distance was selected to calculate clusters in this study. To identify the impact of different air masses in a multiple linear regression model, WRF-FLEXPART (Stohl et al., 2005; Brioude et al., 2013) was



used to obtain the clusters of particle trajectories reaching the Nam Co Station. 1000 particles were released per hour in the
 115 bottom 100 m surface layer above Nam Co Station and were tracked in backward mode for 4 days (de Foy et al., 2016a).
 Residence Time Analysis (RTA) (Ashbaugh et al., 1985) was used to show the dominant transport paths of air masses impacting
 the samples (Wang et al., 2016; Wang et al., 2017). Six clusters were found to represent the dominant flow patterns to the Nam
 Co Station.

2.4 Multiple Linear Regression Model

120 A Multiple Linear Regression (MLR) model was used in this study to quantify the main factors affecting maximum daily
 8-hour average surface ozone concentrations. The method follows the description provided in de Foy et al. (2016b and 2016c).
 The inputs to the MLR model include meteorological parameters, interannual variation factors, seasonal factors and WRF-
 FLEXPART trajectory clusters. To obtain a normal distribution, the MLR model was applied to the logarithm of the ozone
 concentration offset by 10 ppb. The inputs to the model were normalized linearly. An Iteratively Reweighted Least Squares
 125 (IRLS) procedure was used to screen for outliers. Measurement times when the model residual was greater than two standard
 deviations of all the residuals were excluded from the analysis. This was repeated iteratively until the method converged on a
 stable set of outliers. The variables to be included in the regression were obtained iteratively. At each iteration, the variable
 leading to the greatest increase in the square of Pearson's correlation coefficient was added to the inputs as long as the increase
 was greater than 0.005.

130 2.5 Potential Source Contribution Function

The Potential Source Contribution Function (PSCF) assumes that back-trajectories arriving at times of higher mixing
 ratios likely point to the more significant source directions (Ashbaugh et al., 1985). PSCF has been applied in previous studies
 to locate sources of surface ozone for different sites (Kaiser et al., 2007; Dimitriou and Kassomenos, 2015). The PSCF values
 for the grid cells in the study domain are based on a count of the trajectory segment (hourly trajectory positions) that terminate
 135 within each cell (Ashbaugh et al., 1985). Let n_{ij} be the total number of endpoints that fall in the ij th cell during whole simulation
 period. Let m_{ij} represents the number of points in the same cell that have arrival times at the sampling site corresponding to
 surface ozone mixing ratios higher than a set criterion. In this study, we calculate the PSCF based on trajectories corresponding
 to concentrations that exceed the mean level of surface ozone. The PSCF value for the ij th cell is then defined as:

$$\text{PSCF}_{ij} = \frac{m_{ij}}{n_{ij}}$$



The PSCF value can be interpreted as the conditional probability that the ozone mixing ratios at measurement site is greater than the mean mixing ratios if the air parcel passes through the ij th cell before arriving at the measurement site. In cells with high PSCF values are associated with the arrival of air parcels at the receptor site that have pollutant mixing ratios that exceed the criterion value. These cells are indicative of areas of ‘high potential’ contributions for the chemical constituent.

Identical $PSCF_{ij}$ values can be obtained from cells with very different counts of back-trajectory points (eg. grid cell A with $m_{ij}=5000$ and $n_{ij}=10000$ and grid cell B with $m_{ij} = 5$ and $n_{ij} = 10$). In this extreme situation grid cell A has 1000 times more air parcels passing through than grid cell B. Because of the sparse particle count in grid cell B, the PSCF values are more uncertain. To account for the uncertainty due to low values of n_{ij} , the PSCF values were scaled by a weighting function W_{ij} (Polissar et al., 1999). The weighting function reduced the PSCF values when the total number of the endpoints in a cell was less than about three times the average value of the end points per each cell. In this case, W_{ij} was set as follows:

$$W_{ij} = \begin{cases} 1.00 & n_{ij} > 3N_{ave} \\ 0.70 & 3N_{ave} > n_{ij} > 1.5N_{ave} \\ 0.42 & 1.5N_{ave} > n_{ij} > N_{ave} \\ 0.05 & N_{ave} > n_{ij} \end{cases}$$

where N_{ave} represents the mean n_{ij} of all grid cells. The weighted PSCF values were obtained by multiplying the original PSCF values by the weighting factor.

3 Surface ozone behavior at Nam Co Station

3.1 Mean mixing ratio

The mean surface ozone mixing ratio at Nam Co Station during the entire observational period was 47.6 ± 11.6 ppb, and the yearly average surface ozone mixing ratio was between 46.0 and 48.9 ppb (Table 1). During the whole monitoring period, the lowest hourly mixing ratio at Nam Co Station was 10.1 ppb, which was observed on December 3rd 2011, and the highest hourly mixing ratio was 94.7 ppb, which was recorded on June 11th 2011, resulting in a range of ~85 ppb.

The mean surface ozone mixing ratio at Nam Co Station was within the reference range reported for the Himalayas and Tibetan Plateau, and it was higher than the ratios for the two nearest urban sites: Lhasa (Ran et al., 2014) and Dangxiong (Lin et al., 2015); and lower than those of two sites on the edge of the Tibetan Plateau: Waliguan Station (Xu et al., 2011) and NCO-P (5079 m) (Cristofanelli et al., 2010) (see Fig. 1 for station locations). Compared with the surface ozone at background sites in the wider Northern Hemispheric scale (range 20–45 ppb; Vingarzan, 2004), mean surface ozone mixing ratio at Nam Co Station was at high levels over the mid-latitudes sites.



165 3.2 Seasonal pattern

Every month considered in this study had more than 400 hours of available data. The overall trends of surface ozone at Nam Co Station showed similar annual cycles with slight variations (Fig. S1). The monthly average mixing ratios of ozone from 2011 to 2015 at Nam Co Station showed clear seasonal features (Fig. 2): 1) remarkably high values in late spring-early summer; 2) low values in winter; 3) little fluctuation during the remainder of the year except for late spring-early summer and 4) a small peak around October. Three winter months (December, January and February) had the lowest monthly mean surface ozone mixing ratios (41.0 ± 7.6 ppb – 41.5 ± 7.0 ppb) of the year, with variations smaller than 0.5 ppb. Mean surface ozone mixing ratios increased from February to March by ~ 3.5 ppb, and a sharp increase from 44.5 ± 10.4 ppb to 54.7 ± 11.6 ppb occurred in March-April. The mixing ratios remained above 54 ppb for the next 3 months (April, May and June), with the highest mixing ratios occurring in May (58.6 ± 12.2 ppb). After a large decrease in June-July (from 55.5 ± 12.7 ppb to 44.9 ± 11.9 ppb), the surface ozone mixing ratios during the second half of the year remained at low levels (ranging from 41.5 ± 7.0 ppb to 48.0 ± 8.6 ppb), with a small increase in October.

3.3 Diurnal variation

The diurnal cycles at Nam Co Station showed low ozone mixing ratios at night and high ozone mixing ratios during the day, with a unimodal pattern (Fig. 3). After a rapid increase during the morning (8:00-11:00) of 6 ppb, the surface ozone mixing ratio at Nam Co continued to increase until reaching a maximum at 18:00 (53.2 ± 10.9 ppb); it then decreased continuously to its lowest level at 8:00 the next day. Field observations revealed that the ozone mixing ratios reached an average of 50.6 ± 10.9 ppb during the day (9:00-20:00) and an average of 44.6 ± 11.2 ppb during the night and early morning (21:00-8:00). The transition between high levels during the daytime and low levels during the nighttime was fast.

All seasons displayed similar diurnal ozone mixing ratio cycles at Nam Co Station (Fig. 4). The diurnal cycle shift from low level at night to high level during the daytime was generally characterized by early shifts in spring and summer and late shifts in winter, which was most likely related to seasonal differences in sunrise times. Relatively large diurnal amplitudes were observed in spring, with much smaller diurnal amplitudes observed during summer, autumn and winter.

4 Factors affecting surface ozone variation at Nam Co Station

4.1 Stratospheric intrusions

As most of the ozone in the atmosphere is found in the stratosphere, surface ozone may be affected by total column ozone variation and stratospheric intrusions in specific sites (Cristofanelli et al., 2010; Ma et al., 2014). Comparing the correlations



coefficients between maximum 8-hr daily average observed surface ozone, total column ozone, potential vorticity and a WRF-FLEXPART tracer for particles transported to the surface from a height of 8000 m above sea level (Fig. S2), it seems that annual surface ozone did not have an obvious correlation with the other three parameters. ³⁵S results (Lin et al., 2016) also support this result by showing that in the spring; Nam Co was affected by aged stratospheric air originating over the Himalayas rather than being affected by transport from fresh stratospheric air masses directly above Nam Co Station.

4.2 Multiple linear regression model result

A multiple linear regression model was used to quantify the contributions of various factors (including temperature, clear-sky solar radiation, potential vorticity, wind speed, humidity, annual cycle, interannual variation and WRF-FLEXPART trajectory clusters) to the measured maximum daily 8-hour average surface ozone. Comparing the observed surface ozone mixing ratios and the model surface ozone mixing ratios (Fig. 5), the R^2 between model and observation was 0.51 (Fig. S3).

Three factors contributed 97% of the observed variance in the multiple linear regression analysis (Table 2). Clear-sky solar radiation was the largest contributor (72% Table 2) followed by specific humidity and WRF-FLEXPART cluster 4. The contribution of clear-sky solar radiation is in agreement with the strong correlation between monthly mean observed SWD and surface ozone concentration at Nam Co Station in 2012 (Fig. 6). The Pearson's correlation coefficient between monthly SWD and surface ozone was ~ 0.93 for the whole year. Both the MLR model result and SWD observation indicate that most of the surface ozone variability at Nam Co Station is a function of variation in the clear sky solar radiation. Increased solar radiation promoted the photochemical production of surface ozone in spring, which is similar to the mechanism at other background sites (Monks 2000). Specific humidity was the second largest contributor (20%; Table 2) with a negative coefficient indicating that higher surface ozone was associated with drier conditions possibly due to transport of continental air masses; or impacts from air masses aloft. The WRF-FLEXPART trajectory cluster passing by Lhasa and Dangxiong from the south (Cluster 4, Fig. S4) was the third largest contributor (4%; Table 2). The negative coefficient indicates that air masses transported from the south to Nam Co were associated with lower surface ozone. For the whole measurements period, it seems that transport of surface ozone is not the main influencing factor to the daily surface ozone variations in the multiple linear regression model.

4.3 Impact of photochemical production and vertical mixing on diurnal variation

SWD showed a positive correlation with surface ozone (correlation coefficient=0.77) which indicated that the potential of local ozone formation by photochemical production during the daytime contributed to the peak in the afternoon (Wang et al., 2006). The variations of SWD lead to the variations of other meteorological parameters like wind speed and PBLH. Wind



speed and PBLH are also generally regarded as the main factors influencing the diurnal cycle of surface ozone. High wind
220 speed was found to covary with turbulent downward mixing in previous studies in the Tibetan Plateau (Tang et al., 2002; Ma
et al., 2014; Lin et al., 2015). Moreover, PBLH can also be used to represent the vertical mixing intensity in the troposphere.
Hourly average wind speed and PBLH at Nam Co Station showed positive correlation with hourly average surface ozone (Fig.
7). The correlation coefficient between surface ozone and wind speed was 0.95 and the correlation coefficient between surface
ozone and PBLH was 0.92. These results indicate that high surface ozone was associated with high wind speed and high PBLH.

225 The diurnal cycles of surface ozone exhibit similar patterns in different seasons as shown in section 3.3, implying that
similar factors influenced the variation for all seasons. In this study, the diurnal variations of the surface ozone mixing ratios
can largely be explained by solar radiation and vertical mixing which are indicative of in-situ photochemical production with
natural precursors.

5 Synthesis comparison of surface ozone variation across the Tibetan Plateau and beyond

230 5.1 Diurnal variation

Diurnal surface ozone patterns varied among sites across the Tibetan Plateau (Fig. 8). Nam Co Station, Xianggelila, Lhasa
and Dangxiong showed similar diurnal surface ozone patterns as discussed in section 4.3.

235 Diurnal surface ozone at NCO-P showed different patterns in different seasons (Fig. 8), and thermal circulation was the
main influential factor (Cristofanelli et al., 2010). Surface ozone mixing ratio at Waliguan experienced a minimum around
noon and a maximum at night (Fig. 8), which is indicative of a mountain-valley breeze (local anabatic and catabatic winds)
(Xue et al., 2011). Specifically, more boundary layer air affected Waliguan and resulted in lower surface ozone at noon;
whereas at night, more free tropospheric air increased the surface ozone level (Xu et al., 2011). It should be noted that the
amplitudes in the diurnal variations at Waliguan were much smaller than those at other sites.

In all, diurnal surface ozone variations across the Tibetan Plateau were generally controlled by site-specific
240 meteorological conditions and photochemical production. Sites located in plains or valleys exhibited daytime maxima of ozone
associated with local photochemical production whereas mountain top sites experienced daytime ozone minima associated
with up-slope flow of low-ozone air.

5.2 Seasonal variation

245 The seasonal variation of surface ozone mixing ratios at different sites around the world is influenced by many factors
including: the background surface ozone at the site, stratospheric intrusion, photochemical production, long-range transport of



ozone or its precursors, local vertical mixing and even deposition (Vingarzan, 2004; Ordóñez et al., 2005; Tang et al., 2009; Reidmiller et al., 2009; Cristofanelli et al., 2010; Langner et al., 2012).

Seasonal variation of surface ozone in the Northern Hemisphere can be classified into three broad categories (Fig. 9) depending on the timing of the maximum and minimum ozone mixing ratio:

I) Spring-maximum type. This type has maximum surface ozone concentrations in the spring, with the peak month generally in March, April or May; concentrations are at average levels during the autumn and winter, and reach their lowest level during the summer. There are two reasons that likely explain the spring maximum at sites of this type: the increasing photochemical production contributed by increased solar radiation in spring and the accumulation of NO_x and hydrocarbons during the winter (Monks, 2000; Vingarzan, 2004); and the stratospheric intrusions of ozone (Fishman and Crutzen, 1978; Monks, 2000; Vingarzan, 2004). Sites of this type are located in less-polluted regions or in the free troposphere.

II) Summer-maximum type. This type has a plateau of high surface ozone in spring and summer and a minimum in winter. Sites of this type occur in regions with strong ozone precursor emissions in the summer (such as the central European continent) or in regions where stratospheric intrusion occurs frequently in summer.

III) Double-maximum type. This type has two peaks, one in spring and the other in autumn, and it has its minimum in summer. This type likely results from the intrusion of air masses with low ozone mixing ratios from the ocean or tropical regions in the summer. The driving force of these air masses may be the summer monsoon in these areas.

The seasonal variation of ozone at sites across the Tibetan Plateau can be divided into the Summer-maximum and Spring-maximum type based on the location of the sites:

A) The northern Tibetan Plateau: Summer-maximum type.

In the northern Tibetan Plateau (Waliguan site), surface ozone showed a maximum in summer and a minimum in winter (Fig. 9A). The summer maximum of surface ozone at Waliguan was linked to the impact of a high ozone band between 35°N-45°N over 70°E-125°E (Zhu et al., 2004). Similarly, Qinghai Lake site also showed a maximum in summer (Shen et al., 2014). Horizontal and vertical transports have been regarded as major contributor to surface ozone at these two sites (Zhu et al., 2004; Shen et al., 2014).

B) The central Tibetan Plateau: Spring-maximum type.

Sites in the central Tibetan Plateau including Nam Co Station showed maximum ozone during late spring-early summer



and relatively low levels in the remainder of year (Fig. 9B), corresponding to the Spring-maximum type. Compared with the surface ozone levels at Nam Co Station, those at Lhasa and Dangxiong were much lower. Considering the result of the multiple linear regression model, it is possible that the local NO_x emissions in these two urban regions reduce the average ozone on the urban scale. A study at Dangxiong revealed that the greater rainfall in summer caused the surface ozone levels to remain relatively low during the warm period (July-September) (Lin et al., 2015). At Lhasa, photochemistry was the main factor affecting surface ozone in spring and summer, whereas transport largely contributed to the observed ozone mixing ratios in autumn and winter (Ran et al., 2014). Large-scale background of surface ozone in spring considered an important influence on Dangxiong and Lhasa in spring (Lin et al., 2015; Ran et al., 2014).

C) The southern Tibetan Plateau: Spring-maximum type.

In the southern Tibetan Plateau, NCO-P and Xianggelila each had a single surface ozone peak in spring (pre-monsoon) and a minimum in summer (monsoon) with a difference between the two exceeding 30 ppb. This pattern is different from those of the northern and central Tibetan Plateau (Fig. 9C). At NCO-P, frequent stratospheric intrusions were recorded in all seasons except during the monsoon season (Cristofanelli et al., 2010). A similar frequency of downward transport was identified at Xianggelila, including less frequent intrusions in the summer (Ma et al., 2014).

5.3 Regional representativity of surface ozone at Nam Co Station

Backward trajectories and PSCF were utilized to identify the source of surface ozone at Nam Co Station and to assess the regional representativity of surface ozone at Nam Co. In spring, the air masses that arrived at Nam Co Station were predominantly from the west and from the south, and the 3-D clusters indicated that the air masses traveled through the Himalayas before reaching Nam Co Station (Fig. 10). Cristofanelli et al. (2010), Putero et al. (2016) and Chen et al. (2011) found that the frequency of stratospheric intrusions in the Himalayas was high in spring, and slightly lower than during the winter. This was confirmed by analysis of the ERA-Interim data set showed that the seasonal average ozone flux from the stratosphere to the troposphere in the Himalayas was the highest in spring (Škerlak et al., 2014). As a result, surface ozone was much higher at NCO-P than at Nam Co Station in spring (Cristofanelli et al., 2010). Air masses transported from the Himalayas therefore led to higher concentrations of surface ozone at Nam Co Station.

In the summer, there are more backward trajectories coming from the northern Tibetan Plateau than in the other seasons (Fig. 10). During the summer the northern Tibetan Plateau is the hot spot of stratosphere-to-troposphere ozone flux; and during autumn this flux remains higher than the one in the southern Tibetan Plateau (Škerlak et al., 2014). The summer peak of surface



ozone at Waliguan also suggests that the northern Tibetan Plateau and northwestern China (a band between 35°N-45°N over
300 70°E-125°E) have their highest level of surface ozone in summer (Zhu et al., 2004). HYSPLIT backward trajectories arriving
at Nam Co Station in the summer were classified in 6 clusters. As expected, clusters which came from the northern Tibetan
Plateau had higher mean surface ozone levels than clusters which came from the southern Tibetan Plateau (Fig. 11). The air
masses that arrived at Nam Co Station from the northern Tibetan Plateau and northwestern China by horizontal wind transport
likely resulted in the higher ozone concentrations at Nam Co Station in the summer.

305 Using the PSCF results, we have identified air masses associated with higher surface ozone at Nam Co Station in different
seasons (Fig. 12) and throughout the measurement periods (Fig. S5). The Himalayas region to the south of Nam Co Station
and South Asian countries including Nepal, India Pakistan, Bangladesh and Bhutan had high PSCF weight values in both
spring and summer. The large areas of northwestern China, including the northern Tibetan Plateau, were additional potential
source regions in the summer. The PSCF values at both the southern Tibetan Plateau and the northern Tibetan Plateau in autumn
310 were smaller than those in spring and summer. In autumn, the inland Tibetan Plateau seems to have a larger impact on the
study site than regions more on the edge of the Tibetan Plateau. In winter, no obvious region was identified, which was likely
due to low surface ozone mixing ratios in all these areas.

5.4 Surface ozone at Nam Co as representative of the inland Tibetan Plateau

The atmospheric environment of the Tibetan Plateau and its relationship to regional and global change are of universal
315 concern due to the rapid responses and feedbacks specific to the “Third Pole”. The Tibetan Plateau covers vast areas with
varied topography; however, comprehensive monitoring sites are few and sporadically distributed. Analysis of atmospheric
composition at Waliguan in the north and Everest in the south of the Tibetan Plateau have shown that they are representative
of high-altitude background sites for the entire Tibetan Plateau. It is noteworthy that the Tibetan Plateau, as a whole, is primarily
regulated by the interplay of the Indian summer monsoon and the westerlies; and the atmospheric environment over the Tibetan
320 Plateau is heterogeneous. Mount Everest is representative of the Himalayas on the southern edge of the Tibetan Plateau and is
the sentinel of South Asia where anthropogenic atmospheric pollution has been increasingly recognized as disturbing the high
mountain regions (Decesari et al., 2010; Maione et al., 2011; Putero et al., 2014). In addition, Mount Everest has been identified
as a hotspot for stratospheric- tropospheric exchange (Cristofanelli et al., 2010; Škerlak et al., 2014) where the surface ozone
is elevated from the baseline during the spring due to frequent stratospheric intrusions. Waliguan, in the northern Tibetan
325 Plateau, is occasionally influenced by regional polluted air masses (Zhu et al., 2004; Xue et al., 2011; Zhang et al., 2011). Its
mountainous landform facilitates mountain-valley breezes and may sometimes pump up local anthropogenic emissions



especially during the winter (Xue et al., 2011). Nam Co Station, in the inland Tibetan Plateau, is distant from both South Asia and northwestern China, and its atmospheric environment has been recorded as pristine (Cong et al, 2009). The episodic occurrence of long-range transport of air pollutants from South Asia has been detected at this station (Xia et al, 2011; Lüthi et al., 2015). This occurrence has also been evidenced by the study of aerosol and precipitation chemistry at Nam Co (Cong et al., 2007; Cong et al., 2010).

During the summer, surface ozone concentrations at Nam Co Station are higher than the northern hemisphere average, which suggests that there are impacts of long-range transport. Nam Co is less influenced by stratospheric intrusions than NCO-P on the slopes of Mount Everest, and it is minimally influenced by local anthropogenic emission as evidenced by the constant long-term variation of surface ozone and consistent diurnal variation regardless of season, as discussed above. Therefore, the surface ozone levels and variation at Nam Co can be considered representative of the inland Tibetan Plateau. The levels can serve as essential baseline data to enable a comprehensive understanding of regional and perhaps hemispheric surface ozone variations. Integrated analyses of synchronous monitored indices at Nam Co station and at inter-site comparisons are warranted for further understanding ozone-related climatic and environmental effects over the Tibetan Plateau.

6 Summary

Surface ozone mixing ratios and meteorological parameters were continuously measured from January 2011 to October 2015 at Nam Co Station in the inland Tibetan Plateau. The inter-annual mixing ratios of surface ozone were stable with an average of 47.6 ± 11.6 ppb throughout the monitoring period. Nam Co Station represents a wide background region in the Tibetan Plateau where the baseline of surface ozone is mainly controlled by various natural factors and is minimally disturbed by anthropogenic emissions. The surface ozone mixing ratios at Nam Co Station were high in spring and low in winter. The diurnal cycle indicated that the ozone mixing ratio continued to increase after sunrise until sunset and was higher in the daytime than at night.

Synthesis comparison indicated that Nam Co is less influenced by stratospheric intrusions and anthropogenic disturbances than sites along the rim of the Tibetan Plateau. The seasonality of surface ozone at Nam Co is most similar to other background sites in the Northern Hemisphere, albeit with slightly higher fluctuations in the summer season due to infrequent occurrences of air mass transport from Northwest China. The unique geographical characteristics make Nam Co Station more representative of the baseline of surface ozone in the extensive inland of Tibetan Plateau than other existing monitoring sites.

Our measurements serve as baseline measurements of tropospheric ozone at a remote site in the Tibetan Plateau, and they are expected to expand the understanding of ozone cycles and related physico-chemical and transport processes over the



355 Tibetan Plateau. More long-term measurements of surface ozone at field sites covering the spatially extensive Tibetan Plateau
 are needed for comparison and for integrated studies of ozone cycles in this region.

Acknowledgements

This study was supported by the National Natural Science Foundation of China (41371088, and 41630754) and the
 360 Strategic Priority Research Program (B) of the Chinese Academy of Sciences (XDB03030504).

References

- Ashbaugh, L. L., Malm, W. C., and Sadeh, W. Z.: A residence time probability analysis of sulfur concentrations at Grand Canyon National Park, *Atmospheric Environment* (1967), 19, 1263-1270, 1985.
- 365 Brasseur, G., Orlando, J. J., and Tyndall, G. S.: *Atmospheric chemistry and global change*, Oxford University Press, 1999.
- Brioude, J., Arnold, D., Stohl, A., Cassiani, M., Morton, D., Seibert, P., Angevine, W., Evan, S., Dingwell, A., and Fast, J. D.: The Lagrangian particle dispersion model FLEXPART-WRF version 3.1, *Geoscientific Model Development*, 6, 1889-1904, 2013.
- Chameides, W., and Walker, J. C.: A photochemical theory of tropospheric ozone, *Journal of Geophysical Research*, 78, 8751-
 370 8760, 1973.
- Chen, X., Ma, Y., Kelder, H., Su, Z., and Yang, K.: On the behaviour of the tropopause folding events over the Tibetan Plateau, *Atmospheric Chemistry and Physics*, 11, 5113-5122, 2011.
- Cong, Z., Kang, S., Liu, X., and Wang, G.: Elemental composition of aerosol in the Nam Co region, Tibetan Plateau, during summer monsoon season, *Atmospheric Environment*, 41, 1180-1187, 2007.
- 375 Cong, Z., Kang, S., Smirnov, A., and Holben, B.: Aerosol optical properties at Nam Co, a remote site in central Tibetan Plateau, *Atmospheric Research*, 92, 42-48, 2009.
- Cong, Z., Kang, S., Zhang, Y., and Li, X.: Atmospheric wet deposition of trace elements to central Tibetan Plateau, *Applied Geochemistry*, 25, 1415-1421, 2010.
- Cooper, O. R., Parrish, D., Ziemke, J., Balashov, N., Cupeiro, M., Galbally, I., Gilge, S., Horowitz, L., Jensen, N., and
 380 Lamarque, J.-F.: Global distribution and trends of tropospheric ozone: An observation-based review, *Elementa: Science of the Anthropocene*, 2, 000029, 2014.
- Cristofanelli, P., Bracci, A., Sprenger, M., Marinoni, A., Bonafè, U., Calzolari, F., Duchi, R., Laj, P., Pichon, J., and Roccato, F.: Tropospheric ozone variations at the Nepal Climate Observatory-Pyramid (Himalayas, 5079 m asl) and influence of deep stratospheric intrusion events, *Atmospheric Chemistry and Physics*, 10, 6537-6549, 2010.
- 385 Crutzen, P. J.: Photochemical reactions initiated by and influencing ozone in unpolluted tropospheric air, *Tellus*, 26, 47-57, 1974.



- de Foy, B., Lu, Z., and Streets, D. G.: Impacts of control strategies, the Great Recession and weekday variations on NO₂ columns above North American cities, *Atmospheric Environment*, 138, 74-86, 2016b.
- de Foy, B., Lu, Z., and Streets, D. G.: Satellite NO₂ retrievals suggest China has exceeded its NO_x reduction goals from the
390 twelfth Five-Year Plan, *Scientific Reports*, 6, 2016c.
- de Foy, B., Tong, Y., Yin, X., Zhang, W., Kang, S., Zhang, Q., Zhang, G., Wang, X., and Schauer, J. J.: First field-based atmospheric observation of the reduction of reactive mercury driven by sunlight, *Atmospheric Environment*, 134, 27-39, 2016a.
- Decesari, S., Facchini, M., Carbone, C., Giulianelli, L., Rinaldi, M., Finessi, E., Fuzzi, S., Marinoni, A., Cristofanelli, P., and
395 Duchi, R.: Chemical composition of PM₁₀ and PM₁ at the high-altitude Himalayan station Nepal Climate Observatory-Pyramid (NCO-P) (5079 m asl), *Atmospheric Chemistry and Physics*, 10, 4583-4596, 2010.
- Derwent, R. G., Parrish, D. D., Galbally, I. E., Stevenson, D. S., Doherty, R. M., Young, P. J., and Shallcross, D. E.: Interhemispheric differences in seasonal cycles of tropospheric ozone in the marine boundary layer: Observation - model comparisons, *Journal of Geophysical Research: Atmospheres*, 121, 2016.
- 400 Desqueyroux, H., Pujet, J.-C., Prosper, M., Squinazi, F., and Momas, I.: Short-term effects of low-level air pollution on respiratory health of adults suffering from moderate to severe asthma, *Environmental research*, 89, 29-37, 2002.
- Dimitriou, K., and Kassomenos, P.: Three year study of tropospheric ozone with back trajectories at a metropolitan and a medium scale urban area in Greece, *Science of The Total Environment*, 502, 493-501, 2015.
- Draxler, R. G., Parrish, D. D., Galbally, I. E., Stevenson, D. S., Doherty, R. M., Young, P. J., and Shallcross, D. E.:
405 Interhemispheric differences in seasonal cycles of tropospheric ozone in the marine boundary layer: Observation - model comparisons, *Journal of Geophysical Research: Atmospheres*, 121, 2016.
- Draxler, R. R., and Rolph, G.: HYSPLIT (HYbrid Single-Particle Lagrangian Integrated Trajectory) model access via NOAA ARL READY website (<http://www.arl.noaa.gov/ready/hysplit4.html>). NOAA Air Resources Laboratory, Silver Spring, in, Md, 2003.
- 410 Fishman, J., and Crutzen, P. J.: The origin of ozone in the troposphere, 1978.
- Gilge, S., Plass-Dülmer, C., Fricke, W., Kaiser, A., Ries, L., Buchmann, B., and Steinbacher, M.: Ozone, carbon monoxide and nitrogen oxides time series at four alpine GAW mountain stations in central Europe, *Atmospheric Chemistry and Physics*, 10, 12295-12316, 2010.
- Huang, J., Kang, S., Zhang, Q., Yan, H., Guo, J., Jenkins, M. G., Zhang, G., and Wang, K.: Wet deposition of mercury at a
415 remote site in the Tibetan Plateau: concentrations, speciation, and fluxes, *Atmospheric environment*, 62, 540-550, 2012.
- Junge, C. E.: Global ozone budget and exchange between stratosphere and troposphere, *Tellus*, 14, 363-377, 1962.
- Kaiser, A., Scheifinger, H., Spangl, W., Weiss, A., Gilge, S., Fricke, W., Ries, L., Cemas, D., and Jesenovec, B.: Transport of nitrogen oxides, carbon monoxide and ozone to the alpine global atmosphere watch stations Jungfraujoch (Switzerland), Zugspitze and Hohenpeißenberg (Germany), Sonnblick (Austria) and Mt. Kravavec (Slovenia), *Atmospheric Environment*,
420 41, 9273-9287, 2007.
- Kang, S., Yang, Y., Zhu, L., and Ma, Y.: Modern environmental processes and changes in the Nam Co basin, Tibetan Plateau, in, China: Beijing Meteorological Press, 2011.



- Langner, J., Engardt, M., Baklanov, A., Christensen, J. H., Gauss, M., Geels, C., Hedegaard, G. B., Nuterman, R., Simpson, D., and Soares, J.: A multi-model study of impacts of climate change on surface ozone in Europe, *Atmospheric Chemistry and Physics*, 12, 10423-10440, 2012.
- Li, C., Kang, S., Zhang, Q., and Kaspari, S.: Major ionic composition of precipitation in the Nam Co region, Central Tibetan Plateau, *Atmospheric Research*, 85, 351-360, 2007.
- Lin, M., Horowitz, L. W., Oltmans, S. J., Fiore, A. M., and Fan, S.: Tropospheric ozone trends at Mauna Loa Observatory tied to decadal climate variability, *Nature Geoscience*, 7, 136-143, 2014.
- Lin, M., Zhang, Z., Su, L., Hill - Falkenthal, J., Priyadarshi, A., Zhang, Q., Zhang, G., Kang, S., Chan, C. Y., and Thiemens, M. H.: Resolving the impact of stratosphere - to - troposphere transport on the sulfur cycle and surface ozone over the Tibetan Plateau using a cosmogenic ^{35}S tracer, *Journal of Geophysical Research: Atmospheres*, 121, 439-456, 2016.
- Lin, W., Xu, X., Zheng, X., Dawa, J., Baima, C., and Ma, J.: Two-year measurements of surface ozone at Dangxiong, a remote highland site in the Tibetan Plateau, *Journal of Environmental Sciences*, 31, 133-145, 2015.
- Liu, Y., Wang, Y., Pan, Y., and Piao, S.: Wet deposition of atmospheric inorganic nitrogen at five remote sites in the Tibetan Plateau, *Atmospheric Chemistry and Physics*, 15, 11683-11700, 2015.
- Lüthi, Z., Škerlak, B., Kim, S., Lauer, A., Mues, A., Rupakheti, M., and Kang, S.: Atmospheric brown clouds reach the Tibetan Plateau by crossing the Himalayas, *Atmos. Chem. Phys.*, 15, 1-15, 2015.
- Ma, J., Lin, W., Zheng, X., Xu, X., Li, Z., and Yang, L.: Influence of air mass downward transport on the variability of surface ozone at Xianggelila Regional Atmosphere Background Station, southwest China, *Atmospheric Chemistry and Physics*, 14, 5311-5325, 2014.
- Ma, Y., Kang, S., Zhu, L., Xu, B., Tian, L., and Yao, T.: Roof of the world: Tibetan observation and research platform: Atmosphere-land Interaction over a heterogeneous landscape, *Bulletin of the American Meteorological Society*, 89, 1487-1492, 2008.
- Macdonald, A., Anlauf, K., Leaitch, W., Chan, E., and Tarasick, D.: Interannual variability of ozone and carbon monoxide at the Whistler high elevation site: 2002–2006, *Atmos. Chem. Phys.*, 11, 11431-11446, 2011.
- Maione, M., Giostra, U., Arduini, J., Furlani, F., Bonasoni, P., Cristofanelli, P., Laj, P., and Vuillermoz, E.: Three-year observations of halocarbons at the Nepal Climate Observatory at Pyramid (NCO-P, 5079 m asl) on the Himalayan range, *Atmospheric Chemistry and Physics*, 11, 3431-3441, 2011.
- Mauzerall, D. L., and Wang, X.: Protecting agricultural crops from the effects of tropospheric ozone exposure: reconciling science and standard setting in the United States, Europe, and Asia, *Annual Review of Energy and the Environment*, 26, 237-268, 2001.
- Monks, P. S.: A review of the observations and origins of the spring ozone maximum, *Atmospheric Environment*, 34, 3545-3561, 2000.
- Myhre, G., Shindell, D., Bréon, F.-M., Collins, W., Fuglestedt, J., Huang, J., Koch, D., Lamarque, J.-F., Lee, D., and Mendoza, B.: Anthropogenic and natural radiative forcing, *Climate change*, 423, 2013.
- Nagashima, T., Ohara, T., Sudo, K., and Akimoto, H.: The relative importance of various source regions on East Asian surface ozone, *Atmospheric Chemistry and Physics*, 10, 11305-11322, 2010.



- Ordóñez, C., Mathis, H., Furger, M., Henne, S., Hüglin, C., Staehelin, J., and Prévôt, A.: Changes of daily surface ozone
460 maxima in Switzerland in all seasons from 1992 to 2002 and discussion of summer 2003, *Atmospheric Chemistry and Physics*, 5, 1187-1203, 2005.
- Pochanart, P., Akimoto, H., Kajii, Y., Potemkin, V. M., and Khodzher, T. V.: Regional background ozone and carbon
monoxide variations in remote Siberia/east Asia, *Journal of Geophysical Research: Atmospheres*, 108, 2003.
- Polissar, A., Hopke, P., Paatero, P., Kaufmann, Y., Hall, D., Bodhaine, B., Dutton, E., and Harris, J.: The aerosol at Barrow,
465 Alaska: long-term trends and source locations, *Atmospheric Environment*, 33, 2441-2458, 1999.
- Putero, D., Landi, T., Cristofanelli, P., Marinoni, A., Laj, P., Duchi, R., Calzolari, F., Verza, G., and Bonasoni, P.: Influence
of open vegetation fires on black carbon and ozone variability in the southern Himalayas (NCO-P, 5079 m asl),
Environmental Pollution, 184, 597-604, 2014.
- Putero, D., Cristofanelli, P., Sprenger, M., Škerlak, B., Tositti, L., and Bonasoni, P.: STEFLUX, a tool for investigating
470 stratospheric intrusions: application to two WMO/GAW global stations, *Atmospheric Chemistry and Physics*, 16, 14203-14217, 2016.
- Qiao, Q., and Zhang, Y.: Synoptic meteorology of the Tibetan Plateau and its effect on the near areas, in, China Meteorological
Press, Beijing, 1994.
- Ran, L., Lin, W., Deji, Y., La, B., Tsering, P., Xu, X., and Wang, W.: Surface gas pollutants in Lhasa, a highland city of Tibet–
475 current levels and pollution implications, *Atmospheric Chemistry and Physics*, 14, 10721-10730, 2014.
- Reidmiller, D., Fiore, A. M., Jaffe, D., Bergmann, D., Cuvelier, C., Dentener, F., Duncan, B. N., Folberth, G., Gauss, M., and
Gong, S.: The influence of foreign vs. North American emissions on surface ozone in the US, *Atmospheric Chemistry
and Physics*, 9, 5027-5042, 2009.
- Shen, Z., Cao, J., Zhang, L., Zhao, Z., Dong, J., Wang, L., Wang, Q., Li, G., Liu, S., and Zhang, Q.: Characteristics of surface
480 O₃ over Qinghai Lake area in Northeast Tibetan Plateau, China, *Science of the Total Environment*, 500, 295-301, 2014.
- Škerlak, B., Sprenger, M., and Wernli, H.: A global climatology of stratosphere–troposphere exchange using the ERA-Interim
data set from 1979 to 2011, *Atmos. Chem. Phys.*, 14, 913-937, 2014.
- Stohl, A., Forster, C., Frank, A., Seibert, P., and Wotawa, G.: Technical note: The Lagrangian particle dispersion model
FLEXPART version 6.2, *Atmospheric Chemistry and Physics*, 5, 2461-2474, 2005.
- Tang, G., Li, X., Wang, Y., Xin, J., and Ren, X.: Surface ozone trend details and interpretations in Beijing, 2001–2006,
485 *Atmospheric Chemistry and Physics*, 9, 8813-8823, 2009.
- Tang, J., Zhou, L., Zheng, X., Zhou, X., Shi, G., and Suolang, D.: The observational study of surface ozone at Lhasa suburb
in summer 1998, *Act. Meteo. Sinica*, 60, 221-229, 2002.
- Tarasova, O., Senik, I., Sosonkin, M., Cui, J., Staehelin, J., and Prévôt, A.: Surface ozone at the Caucasian site Kislovodsk
490 High Mountain Station and the Swiss Alpine site Jungfraujoch: data analysis and trends (1990–2006), *Atmos. Chem.
Phys.*, 9, 4157-4175, 2009.
- Vecchi, R., and Valli, G.: Ozone assessment in the southern part of the Alps, *Atmospheric Environment*, 33, 97-109, 1998.
- Vingarzan, R.: A review of surface ozone background levels and trends, *Atmospheric Environment*, 38, 3431-3442, 2004.



- 495 Wang, T., Wei, X., Ding, A., Poon, S. C., Lam, K., Li, Y., Chan, L., and Anson, M.: Increasing surface ozone concentrations in the background atmosphere of Southern China, 1994-2007, *Atmospheric Chemistry and Physics*, 2009.
- Wang, T., Wong, H., Tang, J., Ding, A., Wu, W., and Zhang, X.: On the origin of surface ozone and reactive nitrogen observed at a remote mountain site in the northeastern Qinghai - Tibetan Plateau, western China, *Journal of geophysical research: atmospheres*, 111, 2006.
- 500 Wang, Y., de Foy, B., Schauer, J. J., Olson, M. R., Zhang, Y., Li, Z., and Zhang, Y.: Impacts of regional transport on black carbon in Huairou, Beijing, China, *Environmental Pollution*, 221, 75-84, 2017.
- Wang, Y., Zhang, Y., Hao, J., and Luo, M.: Seasonal and spatial variability of surface ozone over China: contributions from background and domestic pollution, *Atmospheric Chemistry and Physics*, 11, 3511-3525, 2011.
- 505 Wang, Y., Zhang, Y., Schauer, J. J., de Foy, B., Guo, B., and Zhang, Y.: Relative impact of emissions controls and meteorology on air pollution mitigation associated with the Asia-Pacific Economic Cooperation (APEC) conference in Beijing, China, *Science of The Total Environment*, 571, 1467-1476, 2016.
- Wang, Y.: MeteoInfo: GIS software for meteorological data visualization and analysis, *Meteorological Applications*, 21, 360-368, 2014.
- Wu, S., Mickley, L. J., Jacob, D. J., Logan, J. A., Yantosca, R. M., and Rind, D.: Why are there large differences between models in global budgets of tropospheric ozone?, *Journal of Geophysical Research: Atmospheres*, 112, 2007.
- 510 Xia, X., Zong, X., Cong, Z., Chen, H., Kang, S., and Wang, P.: Baseline continental aerosol over the central Tibetan plateau and a case study of aerosol transport from South Asia, *Atmospheric environment*, 45, 7370-7378, 2011.
- Xu, W., Lin, W., Xu, X., Tang, J., Huang, J., Wu, H., and Zhang, X.: Long-term trends of surface ozone and its influencing factors at the Mt Waliguan GAW station, China-Part 1: Overall trends and characteristics, *Atmospheric Chemistry and Physics*, 16, 6191-6205, 2016.
- 515 Xu, X., Tang, J., and Lin, W.: The trend and variability of surface ozone at the global GAW station Mt. WALIGUAN, China, Second Tropospheric Ozone Workshop Tropospheric Ozone Changes: Observations, state of understanding and model performances", WMO/GAW report, WMO, Geneva, 2011, 49-55.
- 520 Xue, L., Wang, T., Zhang, J., Zhang, X., Poon, C., Ding, A., Zhou, X., Wu, W., Tang, J., and Zhang, Q.: Source of surface ozone and reactive nitrogen speciation at Mount Waliguan in western China: new insights from the 2006 summer study, *Journal of geophysical research: atmospheres*, 116, 2011.
- Yao, T., Thompson, L. G., Mosbrugger, V., Zhang, F., Ma, Y., Luo, T., Xu, B., Yang, X., Joswiak, D. R., and Wang, W.: Third pole environment (TPE), *Environmental Development*, 3, 52-64, 2012.
- 525 Zhang, F., Zhou, L., Novelli, P., Worthy, D., Zellweger, C., Klausen, J., Ernst, M., Steinbacher, M., Cai, Y., and Xu, L.: Evaluation of in situ measurements of atmospheric carbon monoxide at Mount Waliguan, China, *Atmospheric Chemistry and Physics*, 11, 5195-5206, 2011.
- Zhang, L., Jin, L., Zhao, T., Yin, Y., Zhu, B., Shan, Y., Guo, X., Tan, C., Gao, J., and Wang, H.: Diurnal variation of surface ozone in mountainous areas: Case study of Mt. Huang, East China, *Science of The Total Environment*, 538, 583-590, 2015.
- 530 Zhu, B., Akimoto, H., Wang, Z., Sudo, K., Tang, J., and Uno, I.: Why does surface ozone peak in summertime at Waliguan?, *Geophysical research letters*, 31, 2004.

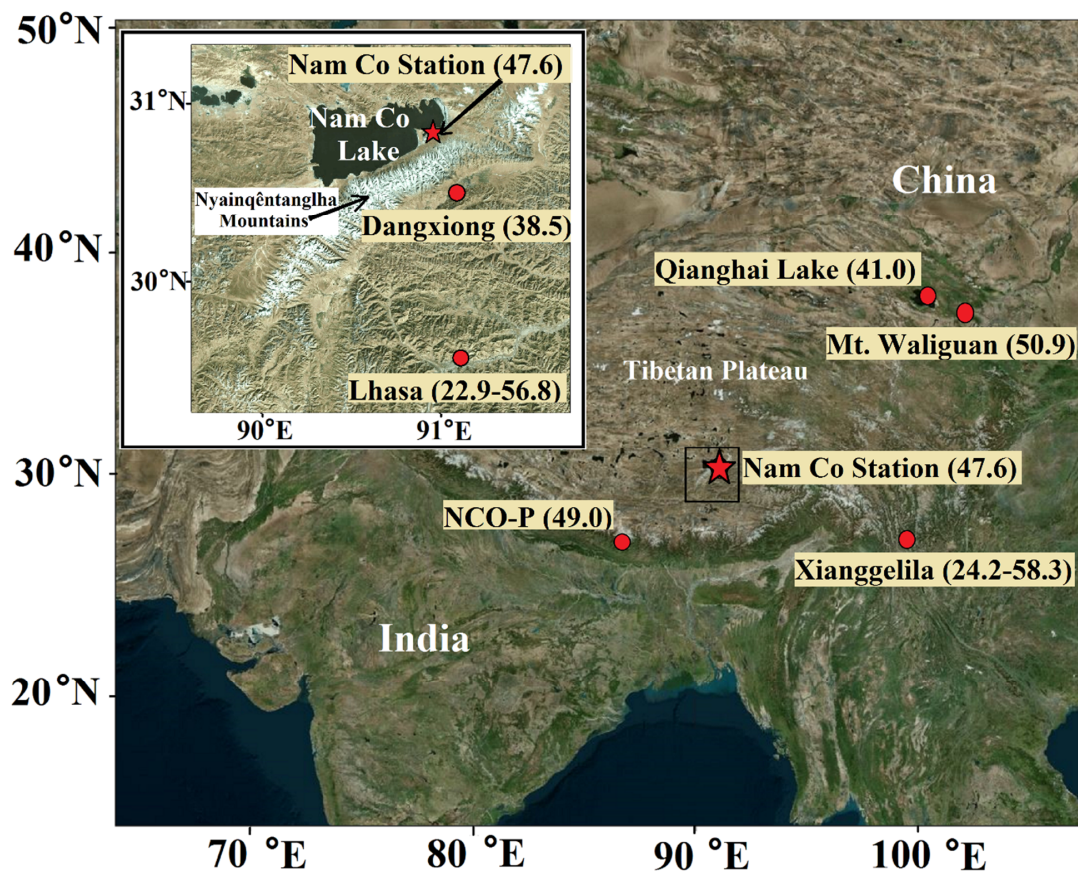


Fig. 1. Geographical location of Nam Co Station and other sites in the Tibetan Plateau. Values in the parenthesis refers to the average or range of surface ozone in ppb as obtained from Cristofanelli et al., 2010; Lin et al., 2015; Shen et al., 2014; Xu et al., 2011; Ma et al., 2014; Ran et al., 2014.

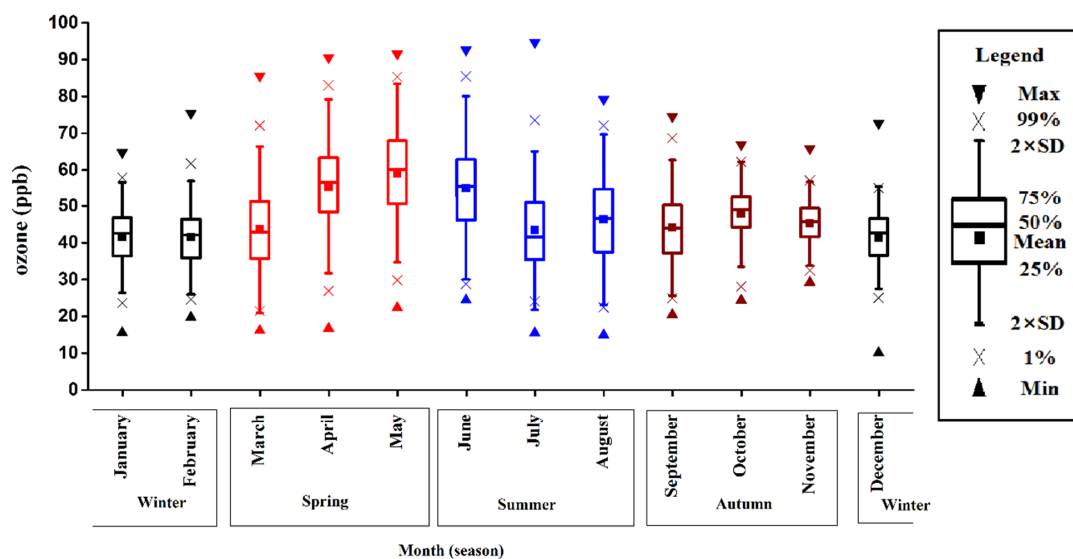


Fig. 2. Monthly average and statistical parameters of surface ozone at Nam Co Station during the whole measurement period (spring (MAM) in red; summer (JJA) in blue; autumn (SON) in dark red; winter (DJF) in black).

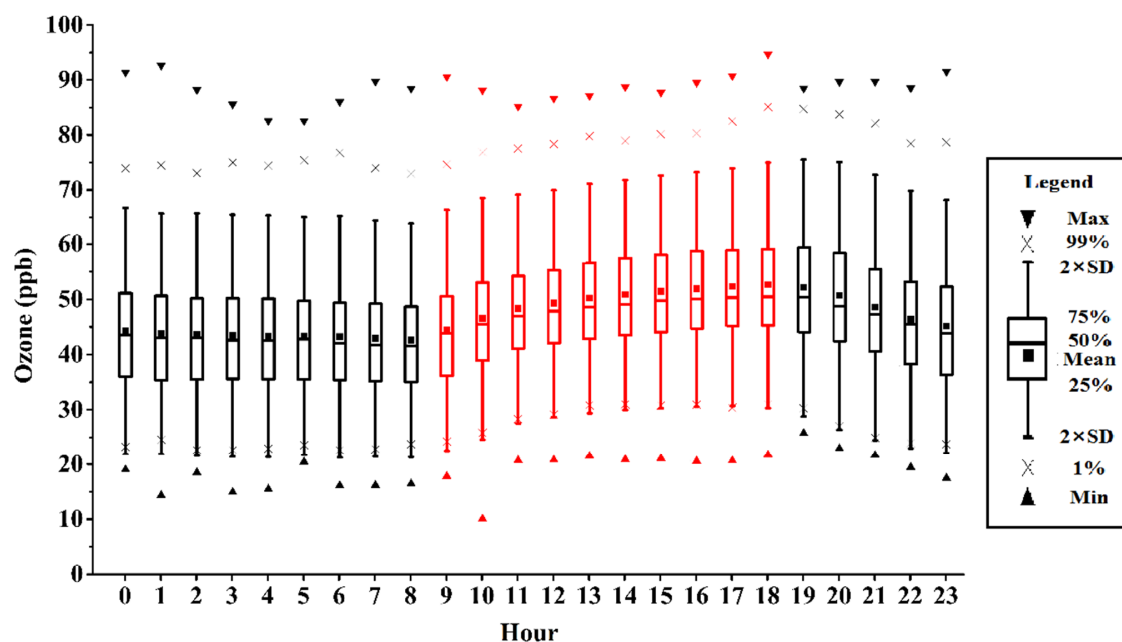


Fig. 3. Diurnal variation of hourly average and statistical parameters of surface ozone at Nam Co Station during the whole measurement period. Boxes during increasing period in red; dots and boxes during decreasing period in black.

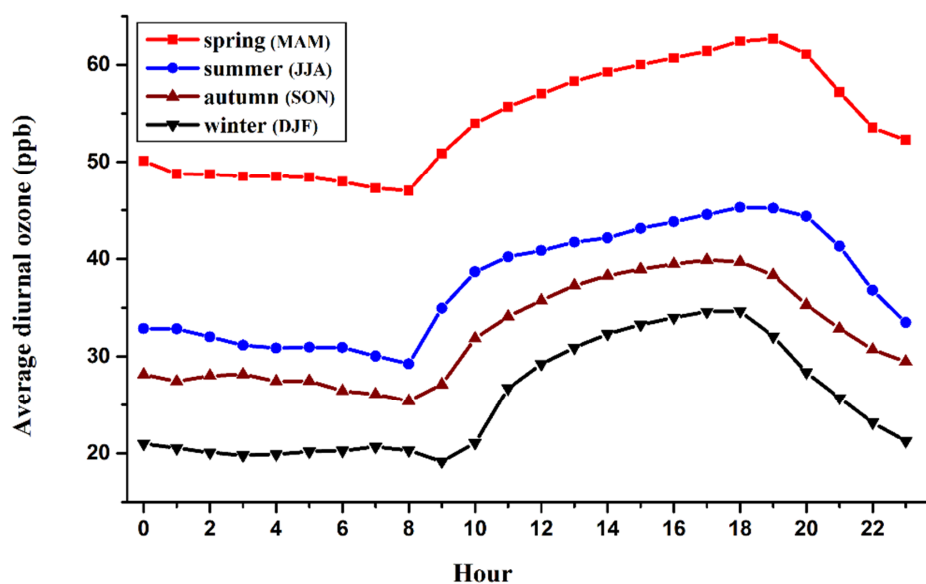


Fig. 4. Diurnal profiles of average hourly surface ozone at Nam Co Station by seasons.

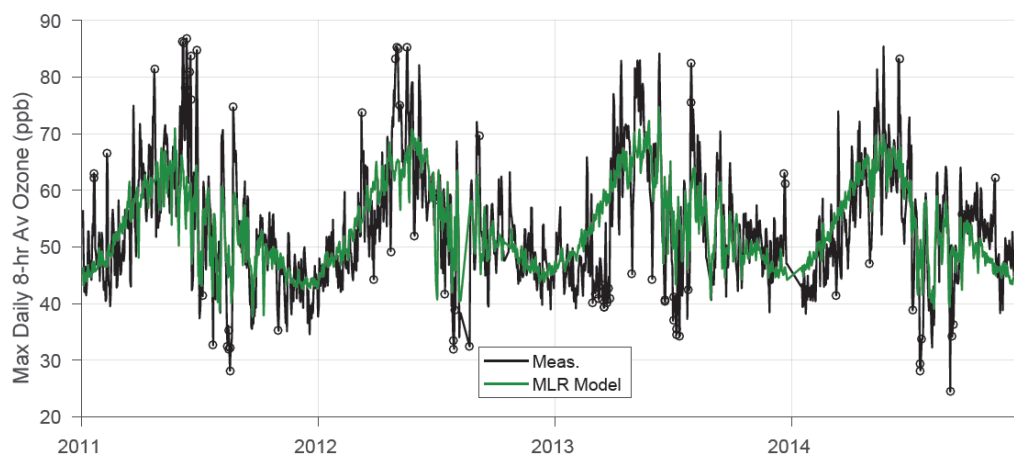


Fig. 5. Comparison between the time series of observed maximum 8-hour daily average surface ozone (black) and multiple linear regression (MLR) model fit (green) at Nam Co Station.

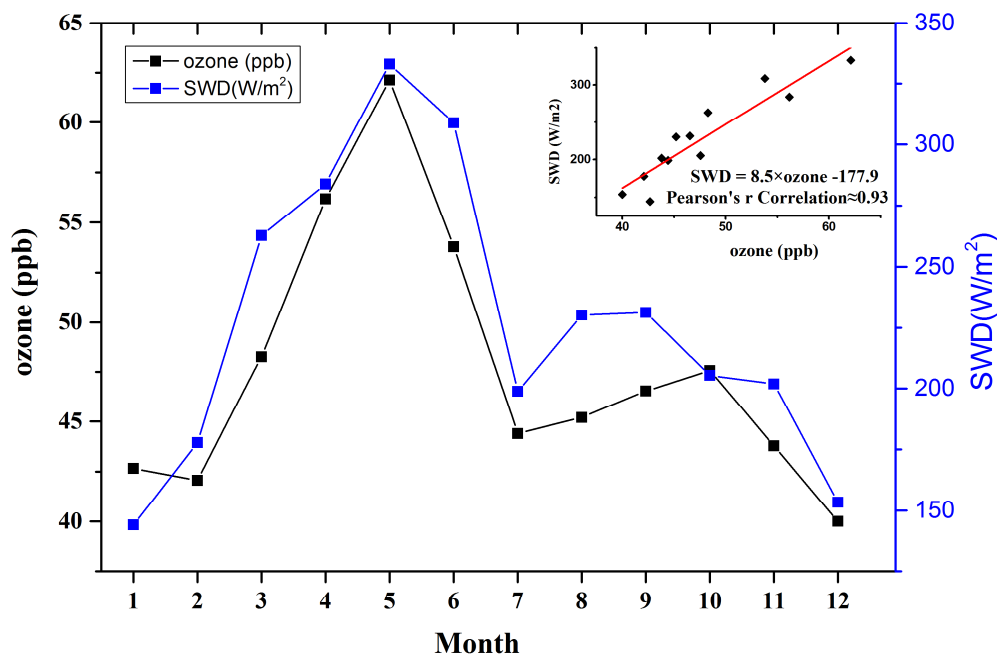


Fig. 6. Comparison between monthly average surface ozone (black) and monthly average SWD (downward shortwave radiation, blue) at Nam Co Station in 2012.

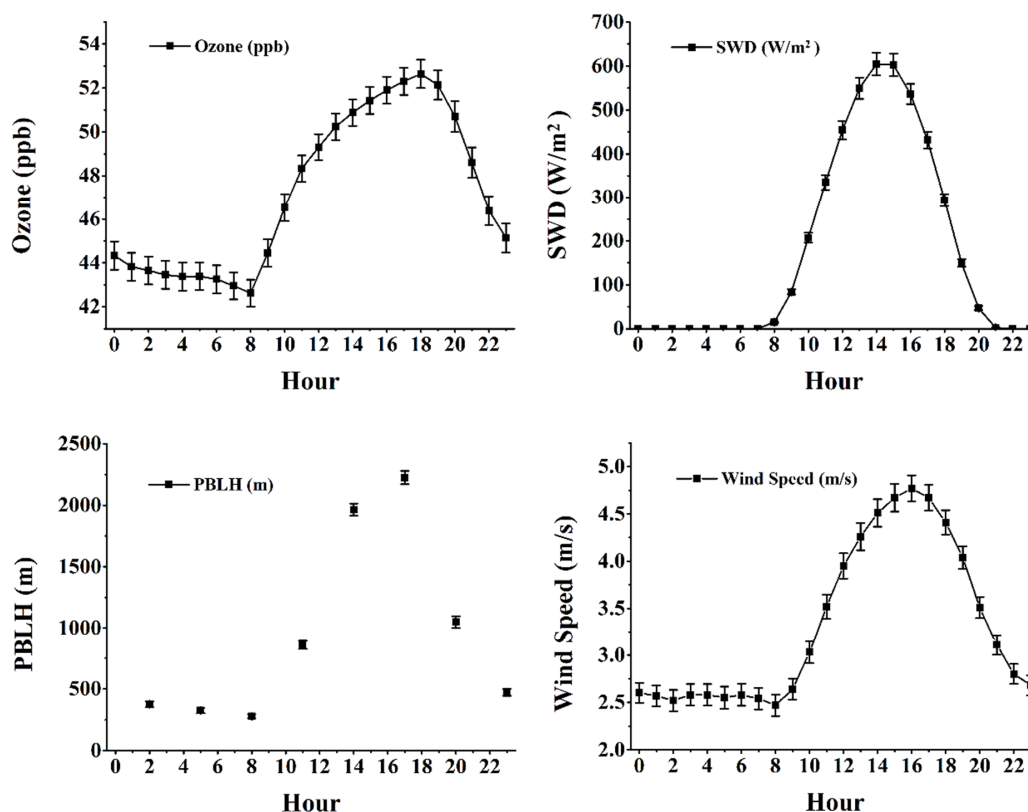


Fig. 7 Diurnal variations of hourly average of surface ozone, SWD (downward shortwave radiation), wind speed and PBLH (planetary boundary layer height) during the whole measurement period at Nam Co Station. Error bars are 95% confidence levels.

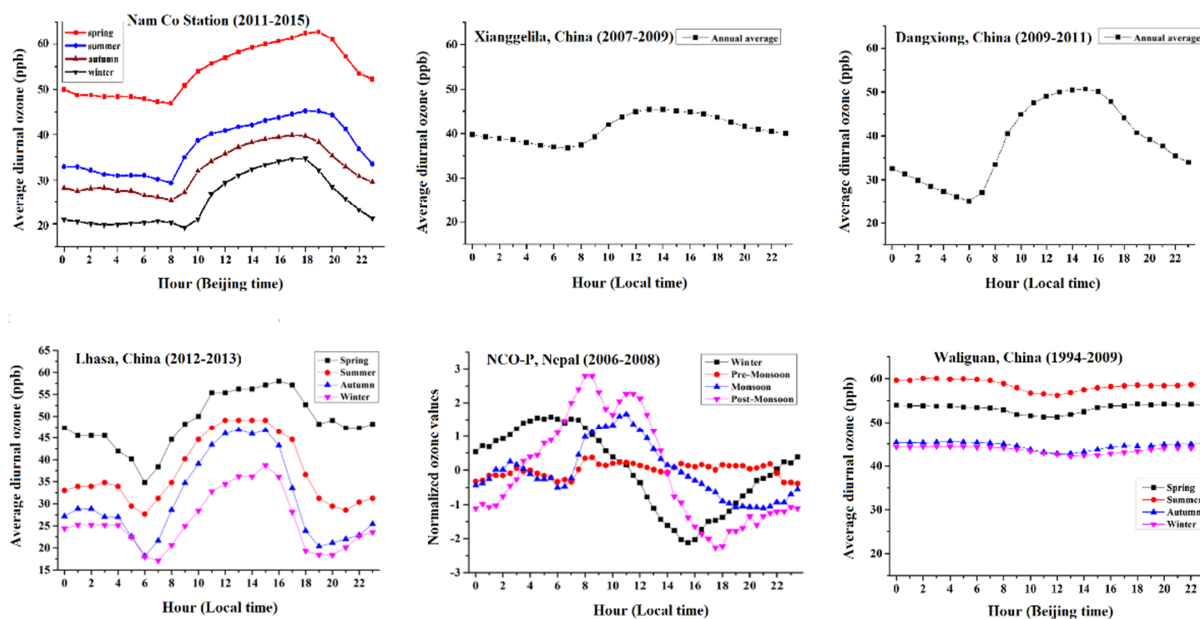


Fig. 8. Comparison of diurnal profiles of surface ozone concentration at different sites in the Tibetan Plateau (referred to Ma et al., 2014; Lin et al., 2015; Ran et al., 2014; Cristofanelli et al., 2010; Xu et al., 2011.) Measurement years at different sites are displayed in brackets.



720

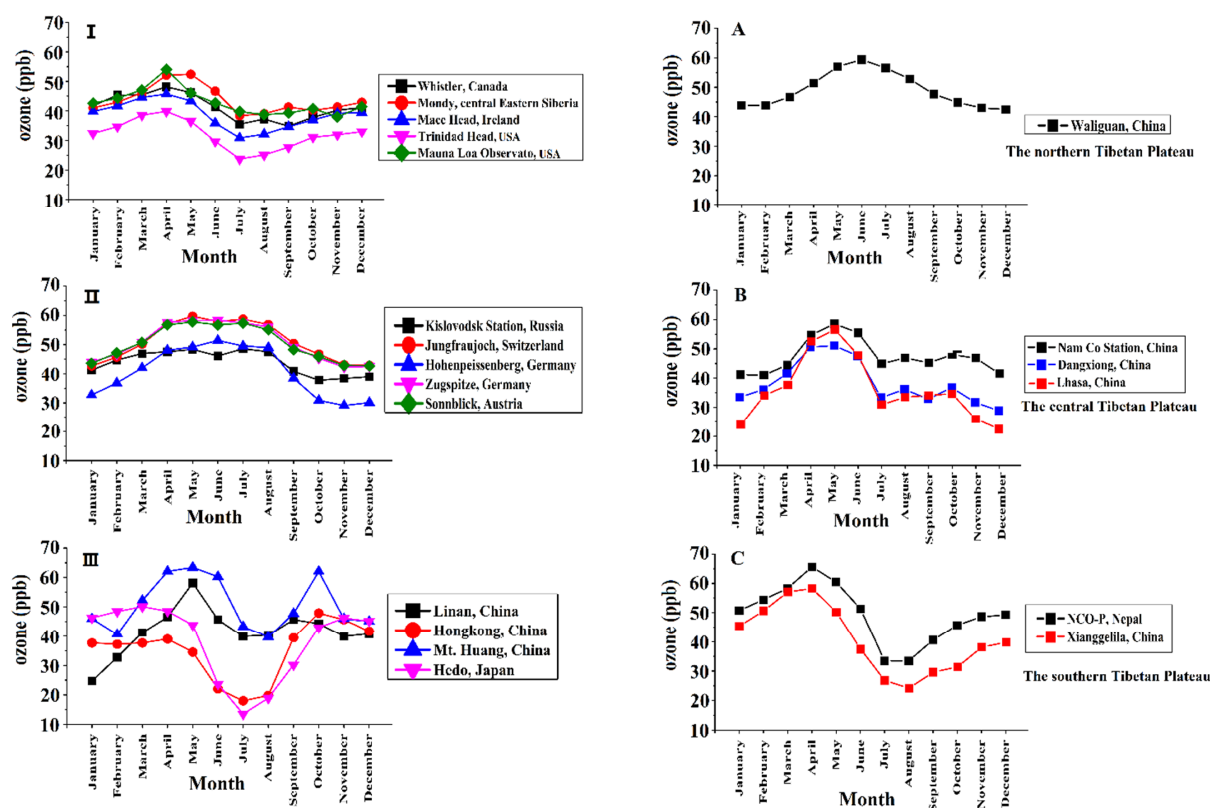


Fig. 9. Three typical types of monthly variations of surface ozone at different sites (left, I : Spring-maximum type; II : Summer-maximum type and III: Double-maximum type.). Monthly variation of surface ozone at different sites in the Tibetan Plateau (right, A: The northern Tibetan Plateau: Summer-maximum type; B: The central Tibetan Plateau: Spring-maximum type and C: The southern Tibetan Plateau: Spring-maximum type) (referred to Ma et al., 2014; Lin et al., 2015; Ran et al., 2014; Cristofanelli et al., 2010; Xu et al., 2011; Macdonald et al., 2011; Pochanart et al., 2003; Derwent et al., 2016; Lin et al., 2014; Tarasova et al., 2009; Gilge et al., 2010; Wang et al., 2011; Wang et al., 2009; Zhu et al., 2004; Zhang et al., 2015; Nagashima et al., 2010).

730

735

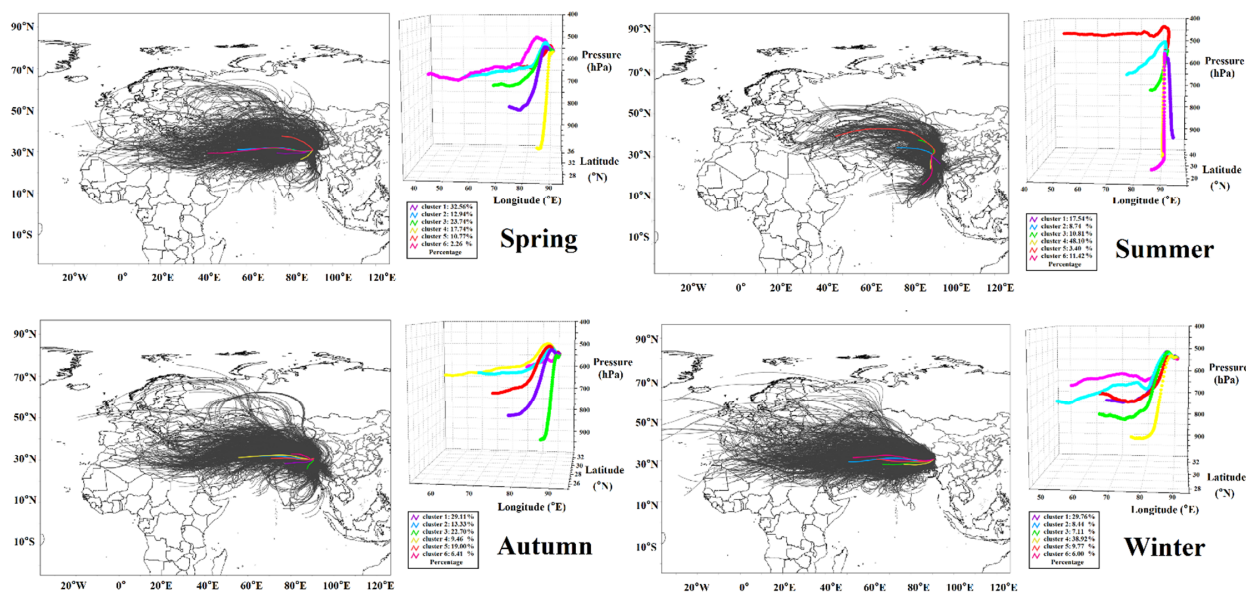


Fig. 10. Backward HYSPLIT trajectories for each measurement day (black lines in the maps), and mean back-trajectory for 6 HYSPLIT clusters (colored lines in the maps, 3D view shown on the right of the maps) arriving at Nam Co Station by season.

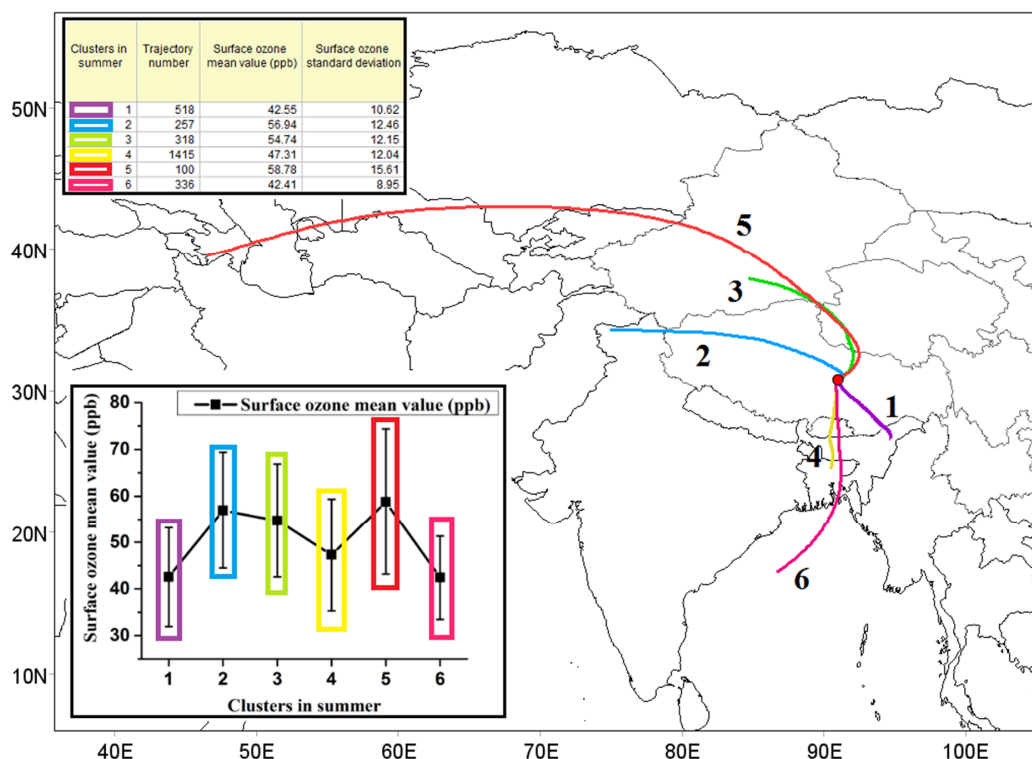


Fig. 11. Mean trajectory of 6 HYSPLIT clusters arriving at Nam Co Station in the summer. Subplot shows the range of surface ozone mixing ratios measured at Nam Co Station by cluster.

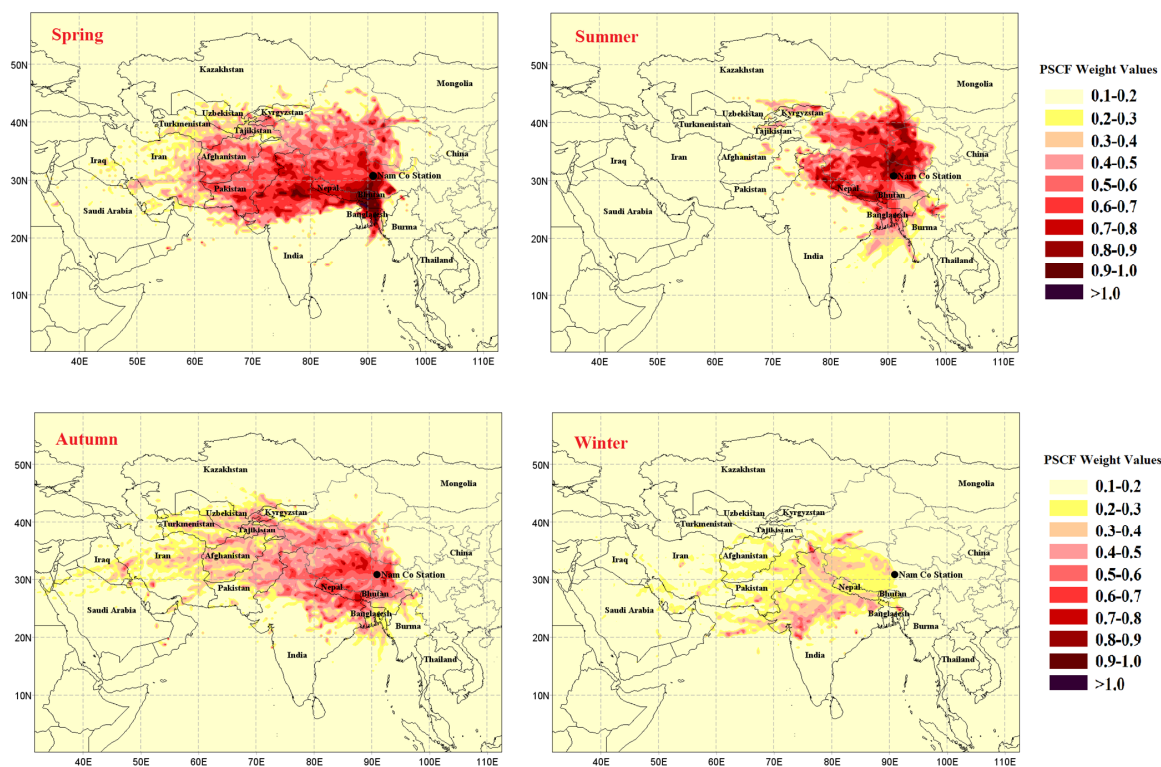


Fig. 12. Likely source areas of surface ozone at Nam Co Station by season identified using PSCF (Potential Source Contribution Function).



810 **Table 1. Statistical summary of surface ozone at Nam Co from 2011 to 2015.**

Year (valid time during whole year %)	Ozone (ppb)	Range (ppb)
2011 (75.25%)	46.0±12.1	10.1-94.7
2012 (90.30%)	48.1±11.4	14.3-91.5
2013 (75.90%)	47.5±12.3	15.5-89.7
2014 (70.05%)	47.5±10.6	14.9-90.8
2015 (66.21%)	48.9±12.0	17.3-94.7
Total	47.6±11.6	10.1-94.7

815

820

825

830

835

840



845

Table 2. Three most important factors determined by the multiple linear regression analysis of the surface ozone at Nam Co Station.

Meteorology	Multiple linear regression factor (%)	Contribution to variability (%)
Clear sky downward shortwave radiation	15.2	72.18
Specific Humidity	-7.5	20.90
WRF-FLEXPART Cluster 4	-16.7	4.36

850

855

860

865

870

875